

Quantum calculation of vortices in the inner crust of neutron stars.

P. Avogadro^{a,b}, F. Barranco^c, R.A. Broglia^{a,b,d}, E. Vigezzi^b

^a Dipartimento di Fisica, Università degli Studi di Milano, via Celoria 16, 20133 Milano, Italy.

^b INFN, Sezione di Milano, via Celoria 16, 20133 Milano, Italy.

^c Departamento de Física Aplicada III, Escuela Superior de Ingenieros, Camino de los Descubrimientos s/n, 41092 Sevilla, Spain.

^d The Niels Bohr Institute, University of Copenhagen, Blegdamsvej 17, 2100 Copenhagen Ø, Denmark.

(Dated: September 22, 2018)

We study, within a quantum mechanical framework based on self-consistent mean field theory, the interaction between a vortex and a nucleus immersed in a sea of free neutrons, a scenario representative of the inner crust of neutron stars. Quantal finite size effects force the vortex core outside the nucleus, influencing vortex pinning in an important way.

PACS numbers: 21.30.Fe Forces in hadronic systems and effective interactions; 26.60.+c Nuclear matter aspects of neutron stars; 95.30.-k Fundamental aspects of astrophysics; 97.60.Jd Neutron stars.

Neutron stars (pulsars) usually rotate with such a precision that they are known as the best timekeepers in the universe. But every so often their rotation rate increases [1]. Anderson and Itoh proposed that these glitches can be viewed as "vorticity jumps", equivalent to "flux jumps" in a superconducting magnet [2].

The density of the neutron star increases going from the surface to the interior, and when it becomes larger than about $n = 5 \times 10^{-4} \text{ fm}^{-3}$, it becomes energetically favourable for some of the neutrons and all of the protons to lump together in extremely neutron rich Sn-like nuclei (that is nuclei containing 40-50 protons and about one hundred neutrons), surrounded by a sea of free neutrons. These nuclei form a pure electrostatic "Wigner" lattice. As one goes deeper into the inner crust, the lattice step decreases, going from about 90 fm at $n = 5 \times 10^{-4} \text{ fm}^{-3}$, to about 30 fm at $n = 7 \times 10^{-2} \text{ fm}^{-3}$. There is strong evidence which testifies to the fact that in this density range, the neutrons are superfluid (cf. e.g.[3,4]). It has been argued that the angular velocity of the superfluid in the inner crust of a neutron star changes either by vortex creep or by vorticity jumps, the latter causing the glitches. Although this scenario has been investigated in a number of publications [5], there remain many open questions associated with the variety of approximations used in these studies. In an effort to shed light into these questions, we report here the first fully quantal, self-consistent calculation of a vortex, taking into account the inhomogeneous character typical of the inner crust of a neutron star.

This allows one to calculate the pinning energy, namely the difference between the energy cost to create a vortex far from the nucleus and on top of it. Our calculations are performed for a single Wigner cell, considering a single nucleus, in keeping with previous estimates [6], which showed that the distance between two neighbouring nuclei of the Coulomb lattice is large compared with typical vortex dimensions, possibly except for the deepest layers of the inner crust.

The calculations were performed solving the Hartree-Fock-Bogoliubov (HFB) equations (often called the De

Gennes equations), within a cylindrical box of radius 30 fm and height 40 fm, imposing that the wavefunctions vanish at the border of the cell. We have assumed that the vortex-nucleus system is axially symmetric (with the vortex directed along the z -axis), but we have constrained the proton density distribution (associated with deeply bound states) to have spherical symmetry.

The De Gennes equations have the form

$$\begin{pmatrix} K + V - E_F & \Delta \\ \Delta & -(K + V - E_F) \end{pmatrix} \begin{pmatrix} U_\alpha \\ V_\alpha \end{pmatrix} = E_\alpha \begin{pmatrix} U_\alpha \\ V_\alpha \end{pmatrix}, \quad (1)$$

and have to be solved simultaneously with the number equation.

The kinetic energy operator (including the effective mass associated with the Skyrme interaction) is denoted by K , $V(\rho, z)$ being the self-consistent Hartree-Fock mean field and Δ the ($S = 0$) pairing field. It displays the functional form

$$\Delta(\rho, z, \phi) = -g[n(\rho, z)] \sum_{\alpha} U_{\alpha} V_{\alpha}^* = \Delta(\rho, z) e^{i\nu\phi}, \quad (2)$$

where ρ is the distance to this axis in the $x - y$ plane and ϕ is the azimuthal angle, while g denotes the density-dependent strength of a (contact) pairing interaction.

Equations (1)-(2) allow for different solutions, which can be labeled by the vortex number ν ($\nu = 0, 1, 2, \dots$). We have mostly considered the $\nu = 1$ case, in which each Cooper pair carries one unit of angular momentum, its projection along the z -axis being $+1$. Note that for $\nu = 0$ one recovers the Negele-Vautherin results [7].

The SkII force [8] was used for determining the HF field, while in the pairing sector we have adopted the density-dependent contact interaction introduced in ref. [9], corresponding to the values $g[n] = -481(1 - (n/n_o)^{0.45}) \text{ MeV fm}^3$, where $n_o = 0.08 \text{ fm}^{-3}$. This interaction reproduces the values of the pairing gap calculated with the Gogny force in uniform neutron matter.

The ϕ dependence of the quasiparticle amplitudes U, V

is

$$U_\alpha(\rho, z, \phi) = U_\alpha(\rho, z)e^{il_\alpha\phi}; V_\alpha(\rho, z, \phi) = V_\alpha(\rho, z)e^{i[l_\alpha - \nu]\phi}. \quad (3)$$

The quasiparticle amplitudes are expanded on a basis of (free) single-particle wavefunctions inside the cylinder

$$U_\alpha(\rho, z) = \sum_{nm} U_\alpha^{n,m} \psi_{n,l_\alpha}(\rho) \chi_m(z), \quad (4)$$

and similarly for V_α (replacing ψ_{n,l_α} with $\psi_{n,l_\alpha - \nu}$). The functions $\chi_m(z)$ are (longitudinal) plane waves and $\psi_{n,l_\alpha}(\rho)$ (radial) Bessel functions, associated with a cylinder with perfectly reflecting walls, l_α being the single-particle angular momentum along the cylinder axis, chosen as quantization axis. To limit computational complexity we have not included the spin-orbit interaction term in the calculation of the single-particle levels. Concerning the protons, we have solved the $\nu = 0$ equations in a spherical box of radius $R_p = 15$ fm, using the same SkII force as for the neutrons. The effect of the neutrons on the (deeply bound) protons, has been included after a spherical average of the various neutron distributions has been carried out.

In what follows we discuss the results associated with the value $E_F = 5.8$ MeV of the Fermi energy. The spatial dependence of the (neutron) density n and of the pairing gap Δ for a nucleus immersed in the neutron sea is shown in Fig. 1. The results for the density essentially coincide with the results of Negele and Vautherin for the corresponding (spherically symmetric) Wigner cell. The radius R of the nucleus is about 7.5 fm, the associated diffusivity being about 0.9 fm. Far from the nucleus the value of the pairing gap is about $\Delta_{unif} \approx 2.2$ MeV, equal to the value obtained in the case of uniform neutron matter with the adopted pairing interaction, while at the nuclear surface $\Delta \approx 1$ MeV. The strong suppression of the pairing gap inside the nucleus is a consequence of the density dependence of the pairing interaction which reflects the behaviour of the 1S_0 phase shift as a function of the relative kinetic energy of the pair of interacting nucleons.

Let us now study the modifications induced on n and Δ by the presence of a vortex. We first discuss the case of free neutrons, a system which mimics, exception made at the edges of the cylinder, uniform neutron matter. In Fig. 3(a) we display the associated pairing gap for the case of a $\nu = 1$ vortex. It is seen that Δ vanishes along the z -axis. For small values of ρ , $\rho < 3 - 4$ fm, the gap increases linearly as a function of ρ . Defining the vortex core as the value of ρ for which $\Delta(\rho_{core}) = \Delta_{unif}/2$, one obtains $\rho_{core} \approx 2$ fm, a value which is similar to that of the correlation length $\xi \approx \hbar v_F / 2\Delta (\approx 5$ fm). For larger values of ρ the gap increases more slowly, gradually approaching the value Δ_{unif} .

Concerning the density distribution (see Fig. 2(a)), an axially symmetric depletion around the vortex axis is observed, with a radius (defined as the value of n at half saturation density) of the order of 3 fm, which is also of

the order of the average distance between particles ($r_s \approx 1.92/k_F \approx 1.02/(E_F/20)^{1/2}$ fm ≈ 3.6 fm). The above results are similar to those found in ref. [10] within the framework of nuclear energy density functional, taking into account the different asymptotic values of the pairing gap (cf. also [11]).

We now turn our attention to the case of a $\nu = 1$ vortex pinned on the nucleus. The associated neutron density and pairing gap are shown in Fig. 2(b) and 3(b). Comparing with the results displayed in Figs. 2(a) and 3(a) respectively, it is seen that both the density depletion around the vortex axis and the vortex core are strongly influenced by the presence of the nucleus. In fact, the vortex is seen to skate on the surface of the nucleus displaying a small penetration length. In other words, the vortex is essentially expelled by the nucleus. The pairing gap at the surface of the nucleus is strongly suppressed, both compared to the case of a isolated nucleus in the absence of the vortex (cf. Fig. 1(b)) and compared to the case of a vortex in uniform (neutron) matter (cf. Fig. 3(a)). In particular, at $\rho \approx 7$ fm (and $z = 0$) Δ displays a value of about 0.5 MeV (Fig. 3(b)), 1 MeV (Fig. 1(b)) and of 2 MeV (Fig. 3(a)), respectively. Furthermore, the presence of the nucleus delays the rise of the pairing gap to its asymptotic value by 5-7 fm as compared to the uniform case (for example, in the $z = 0$ plane, Δ becomes equal to 1.75 MeV at $\rho \approx 11$ fm, compared to $\rho = 6$ fm in the uniform case).

There are two contrasting effects which influence the behaviour of a $\nu = 1$ vortex in the presence of a nucleus and lead to the results discussed above. First, the small (large) value of the pairing gap inside (outside) the nucleus favours pinning, because one saves pairing energy placing the vortex inside the nucleus. Second, to build a $\nu = 1$ vortex inside the nucleus requires the formation of Cooper pairs out of single-particle levels of opposite parity. This is strongly hindered by the spatial quantization associated with finite size nuclear effects which leads to a distribution of levels around the Fermi energy essentially displaying either positive or negative parity (in other words, a very small $\nu = 1 (\pi = (-1)^\nu = -1)$ phase space [12]). The consequences of spatial quantization on a $\nu = 1$ vortex can be further clarified by comparing the correspondent solution of the De Gennes equations with that associated with a $\nu = 2$ vortex (see Figs. 3(c) and (d): note that within the present context the stability or less of this solution is immaterial). It is seen that the pairing gap in the case $\nu = 2$ displays a quadratic, rather than a linear dependence on ρ , reaching the asymptotic value at a larger distances from the z -axis than in the $\nu = 1$ case. It can also be seen that the pairing gap in the case $\nu = 2$ is modified very little by the presence of the nucleus. This is because $\nu = 2$ vortices thrive on a subspace of single-particle levels all displaying essentially the same parity.

We shall now consider the energy associated with the various situations shown above, for the case of a $\nu = 1$ vortex, and calculate the correspondent pinning energy.

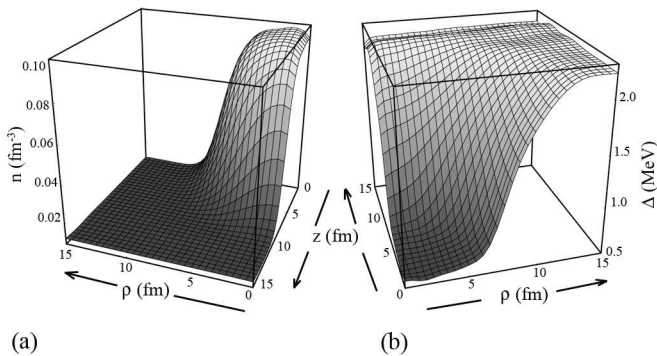


FIG. 1: Density and pairing gap calculated for a nucleus immersed in the neutron sea, at the Fermi energy $E_F = 5.8$ MeV. They are spherically symmetric, but are calculated in the cylindrical box described in the text (radius 30 fm and height 40 fm). Only the region $0 < z < 15$ fm and $0 < \rho < 15$ fm is shown.

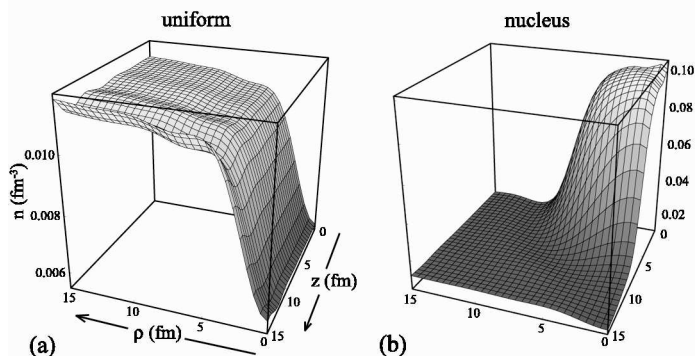


FIG. 2: Density associated with a $\nu = 1$ vortex, calculated in the cylindrical box described in the text (radius 30 fm and height 45 fm), without and with a nucleus at the center of the box. Only the region $0 < z < 15$ fm, $0 < \rho < 15$ fm is shown. (a) Density associated with a $\nu = 1$ vortex in the cell without the nucleus. (b) Density associated with a $\nu = 1$ vortex in the presence of the nucleus.

In our calculation, the energy E_{tot} of a given configuration receives contributions from three sources: the kinetic energy, the mean field potential (HF) energy, and the pairing energy, so that $E_{tot} = E_{kin} + E_{pot} + E_{pair}$. These contributions are displayed in Table 1 for the uniform case (no vortex, no nucleus in the cell: we call the value of the total energy E_U), for an interstitial vortex (no nucleus in the cell, E_I), for an isolated nucleus (no vortex in the cell, E_N), and finally for a vortex pinned on the nucleus (E_P). For the first two cases, our calculation is essentially the same as the one performed in ref. [10], although using a different pairing interaction. The energy cost to create an interstitial vortex or a pinned vortex are given by $E_{IU} = E_I - E_U$ and by $E_{PN} = E_P - E_N$, respectively [13]. In order to be meaningful, the cost to create a vortex should refer to two systems with the same number of neutrons moving in the same box. The cor-

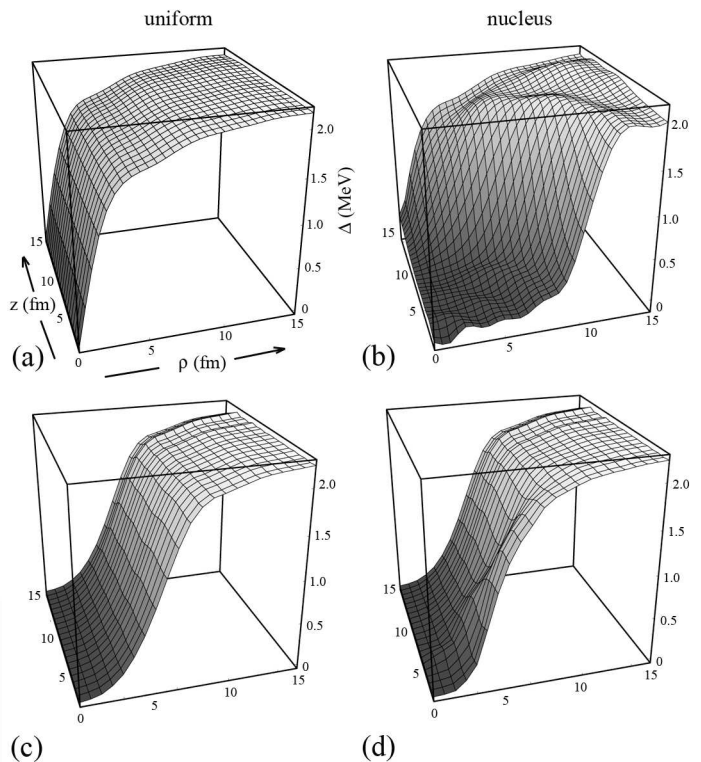


FIG. 3: Pairing gap associated with a $\nu = 1$ and a $\nu = 2$ vortex, calculated in the cylindrical box described in the text (radius 30 fm and height 40 fm), without and with a nucleus at the center of the box. Only the region $0 < z < 15$ fm, $0 < \rho < 15$ fm is shown. (a) Gap associated with a $\nu = 1$ vortex in the cell without the nucleus. (b) Gap associated with a $\nu = 1$ vortex in the presence of the nucleus. (c) Gap associated with a $\nu = 2$ vortex in the cell without the nucleus. (d) Gap associated with a $\nu = 2$ vortex in the presence the nucleus.

	E_{kin}	E_{pot}	E_{pair}	E_{tot}
Uniform	6841.9	-1735.3	-1322.1	3784.5
Vortex, int.	6776.0	-1737.5	-1203.9	3834.6
Nucleus	9971.9	-5784.0	-1274.5	2913.4
Vortex, pinn.	9893.4	-5806.1	-1120.5	2966.8

TABLE I: The total energy E_{tot} , subdivided into the three contributions arising from the kinetic energy E_{kin} , the potential energy E_{pot} and the pairing energy E_{pair} , is shown for each of the four configurations discussed in the text (Wigner cell without the nucleus, cell without the nucleus and with an interstitial vortex, cell with the nucleus, cell with the nucleus and a pinned vortex).

responding solution of the self-consistent equations (1-4) leads to a slight change δE_F of the Fermi energy in going from a system without a vortex to a system with a vortex. For an infinitely large box, the change tends to zero. In the present calculation the change was $\delta E_F \approx 0.05$ MeV.

We have evaluated the error associated with the finite mesh size used in integrating these equations ($\Delta\rho =$

$\Delta z = 0.25$ fm). In particular we have found that the value of the pinning energy, although obtained from the subtraction of large numbers, is remarkably stable with respect to changes in the box size. In fact we estimate that the absolute value of the error associated with this quantity is less than 2 MeV.

The main contribution to $E_{IU} = E_I - E_U$ as reported in Table 1 originates from the pairing energy ($\Delta E_{pair} = 118.2$ MeV), and is associated with the decrease of the pairing field in the region close to the vortex axis (see Fig. 3(a)). At the same time, there is a reduction of kinetic energy due to the reduced population of levels above the Fermi energy. On the other hand, one also expects a positive contribution to the kinetic energy in the presence of a vortex, associated with the irrotational flow around the axis. In the present case the balance turns out to be negative ($\Delta E_{kin} = -65.9$ MeV). The third contribution to E_{IU} arises from a modification in the (HF) mean field. This energy is related to the redistribution of the particles around the vortex, which, in the case under discussion, is small ($\Delta E_{pot} = -2.2$ MeV). Adding the three contributions leads to $E_{IU} = \Delta E_{pair} + \Delta E_{kin} + \Delta E_{pot} = 118.2 - 65.9 - 2.2$ MeV = 50.1 MeV. Analogous considerations can be made to calculate the energy cost E_{PN} to create a vortex pinned on the nucleus. We have in this case $E_{PN} = \Delta E_{pair} + \Delta E_{kin} + \Delta E_{mean} = 154.0 - 78.5 - 22.1$ MeV = 53.4 MeV. It is remarkable that the cost

in pairing energy for a vortex pinned on a nucleus (154.0 MeV) is larger than the cost involved in the creation of a vortex in uniform matter (118.2 MeV). One might have thought that because the vortex tends to lower the pairing gap it would cost less pairing energy to create it in the region occupied by the nucleus, where the pairing gap is lower than in uniform matter (that is, far away from the nucleus, see Fig. 1(b)). However, because the vortex tends to avoid the nucleus, its presence affects the neutron pairing gap essentially only at the nuclear surface. For example, for $z \approx 0, \rho \approx 7$ fm in the uniform case, the pairing gap changes from Δ_{unif} (2.2 MeV, $\nu = 0$ situation) to a value of 1.7 MeV ($\nu = 1$ vortex, cf. Fig. 3(a)). In the pinned case the pairing gap changes from 1.6 MeV ($\nu = 0$ situation) to about 0 MeV ($\nu = 1$ vortex). In other words, the main effect of a vortex in the pinned situation is to zeroth the pairing gap at the nuclear surface, an effect involving an important amount of pairing energy. The pinning energy is defined as the difference between the energy cost to create a pinned vortex, and to create a vortex in uniform matter [6]. For the Fermi energy under consideration ($E_F = 5.8$ MeV) it amounts to $E_{PN} - E_{IU} = 3.3$ MeV [13].

One can conclude that quantal finite size effects, in particular the spatial quantization leading to shell structure, have important effects on the vortex-nucleus interplay.

-
- [1] *The structure and evolution of neutron stars*, D. Pines, R. Tamagaki, S. Tsuruta (eds.), Addison-Wesley, New York (1992).
- [2] P.W. Anderson and N. Itoh, *Nature* **256**(1975)25.
- [3] A. Bohr and B.R. Mottelson, *Nuclear Structure*, Vols. I and II, Benjamin, New York (1969,1975).
- [4] D.M. Brink and R.A. Broglia, *Nuclear Superfluidity*, Cambridge University Press, Cambridge (2005).
- [5] P.W. Anderson et al., *Philos. Mag.* **45**(1982)227; M.A. Alpar, *Astrophys. J.* **213**(1977)527; M.A. Alpar et al., *Astrophys. J.* **278**(1984)791; **346**(1989)823; B. Link et al., *Astrophys. J.* **403**(1993)285; P.B. Jones, *Phys. Rev. Lett.* **79**(1997)792; **81**(1998)4560; *Mon. Not. R. Astron. Soc.* **257**(1998)501; F.V. De Blasio and Ø. Elgaroy, *Phys. Rev. Lett.* **82**(1999)815; P.M. Pizzochero et al., *Phys. Rev. Lett.* **79**(1997)3347; P.M. Donati and P.M. Pizzochero, *Nucl. Phys.* **742A**(2004)363.
- [6] R.I. Epstein and G. Baym, *Astrophys. J.* **328**680(1988).
- [7] J.W. Negele and D. Vautherin, *Nucl. Phys.* **A207**(1973)298.
- [8] D. M. Brink and D. Vautherin, *Phys. Rev.* **C5**(1972)626
- [9] E. Garrido et al., *Phys. Rev.* **C60**(1999)064312
- [10] Y. Yu and A. Bulgac, *Phys. Rev. Lett.* **90**(2003)161101
- [11] Ø. Elgaroy and F.V. De Blasio, *Astronomy & Astrophysics* **370**(2001)939
- [12] It could be argued that spin-orbit interaction, not considered in the present calculation, will shift the relative energies of levels of different parity around the Fermi energy, eventually reducing this effect. However, the S=0 pairing field connects single-particle levels with antiparallel spin projections, which are both either shifted down by the spin-orbit interaction (for $l(1) > 0, s_z(1) > 0; -(l-\nu)(2) < 0, s_z(2) < 0$) or up (for $l(1) > 0, s_z(1) < 0; -(l-\nu)(2) < 0, s_z(2) > 0$). One thus does not expect a significant change of the phase space density relevant for vortex formation.
- [13] To be noted that the energy cost to create a vortex depends linearly on the height of the cylindrical box used for the calculation, and shows a logarithmic divergence with respect to the radius of the box. We have verified that our results obey this geometrical scaling. Such dependences, however, disappear when we consider the pinning energy, which is independent of the box size for sufficiently large boxes.